William G. Bradley, Jr, MD, PhD • David Scalzo, MD[2] • John Queralt, MD
Wolfgang N. Nitz, MS • Dennis J. Atkinson, MS • Priscilla Wong, MD

Normal-Pressure Hydrocephalus: Evaluation with Cerebrospinal Fluid Flow Measurements at MR Imaging[1]

PURPOSE: **To evaluate magnetic resonance (MR) imaging–based quantitative phase-contrast cerebrospinal fluid (CSF) velocity imaging for prediction of successful shunting in patients with normal-pressure hydrocephalus (NPH).**

MATERIALS AND METHODS: **Eighteen patients (mean age, 73 years) with NPH underwent routine MR imaging and CSF velocity MR imaging before ventriculoperitoneal (VP) shunting. The calculated CSF stroke volume and the aqueductal CSF flow void score were compared with the surgical results.**

RESULTS: **All 12 patients with CSF stroke volumes greater than 42 μL responded favorably to CSF shunting. Of the six patients with stroke volumes of 42 μL or less, three improved with shunting while three did not. The relationship between CSF stroke volume greater than 42 μL and favorable response to VP shunting was statistically significant ($P < .05$). There was no statistically significant relationship between aqueductal CSF flow void score and responsiveness to shunting.**

CONCLUSION: **CSF velocity MR imaging is useful in the selection of patients with NPH to undergo shunt formation.**

Index terms: Brain, hydrocephalus, 10.823 • Cerebrospinal fluid, flow dynamics, 10.1214 • Cerebrospinal fluid, MR, 10.1214 • Shunts, ventriculoperitoneal, 10.4513

Radiology 1996; 198:523–529

NORMAL-PRESSURE hydrocephalus (NPH) is characterized by the clinical triad of dementia, gait apraxia, and urinary incontinence, as well as normal opening pressure at lumbar puncture. Findings of imaging studies demonstrate ventriculomegaly out of proportion to cortical sulcal enlargement. Since it was first described in 1965 (1,2), NPH and treatment of it by means of cerebrospinal fluid (CSF) shunting have been the focus of much investigation. The reported success of CSF diversion in treatment of NPH has varied considerably (3–7); the mean rate of improvement is only 50% (8). Prediction of surgical outcome has been attempted by using clinical signs and symptoms (6,9–11), findings of tests of CSF dynamics (eg, CSF pressure recording) (12), response to intrathecal saline infusion (13,14), response to CSF drainage (9,15), findings of imaging studies (such as radiography of the cisterns after administration of radionuclides [16,17], computed tomography [13,18], and radiography of the cisterns after administration of metrizamide [19]), and cerebral blood flow measurements (20–24).

Unfortunately, conflicting reports of the prediction of efficacy with many of these variables have been published, and no clearly useful criteria for selecting patients with NPH to undergo shunt formation have been identified.

Recently, magnetic resonance (MR) imaging has shown great promise toward this end. In particular, a prominent CSF flow void within the aqueduct on proton-density–weighted images has been correlated with a positive response to CSF diversion, while a normal flow void has been linked to a negative response (25). However, the appearance of the flow void is highly dependent on the acquisition parameters used, as well as on the technical characteristics of the MR imaging systems (eg, gradient strength). In addition, evaluation of the flow void is subjective, and common use of gradient moment nulling or "flow compensation" makes the flow void more difficult to evaluate, possibly rendering the flow void a less sensitive predictor than was originally reported for non–flow-compensated images (25).

Table 1
CSF Study Results and Response to Shunt

Patient No./ Age (y)/ Sex	Initial MR Imaging Results: Flow Void Score	Initial MR Imaging Results: CSF Stroke Volume (μL)	Response to Shunt
1/76/F	3	154	+
2/70/F	1	26	+
3/78/F	2	106	+
4/77/F	1	38	+
5/72/F	1	58	+
6/80/M	3	258	+
7/68/F	3	40	+
8/83/M	2	82	+
9/76/M	1	18	−
10/69/F	2	92	+
11/77/M	4	42	−
12/72/F	4	208	+
13/75/F	1	70	+
14/80/F	4	352	+
15/73/M	2	70	+
16/71/F	3	48	+
17/54/M	3	92	+
18/69/M	1	38	−

Note.—+ = positive response, − = negative response.

[1] From the Long Beach Memorial Medical Center, Memorial MRI Center, 403 E Columbia St, Long Beach, CA 90806 (W.G.B., J.Q.); the Department of Radiological Sciences, University of California, Irvine, Orange (D.S., P.W.); and Siemens Medical Systems, Iselin, NJ (W.N.N., D.J.A.). Received June 7, 1995; revision requested July 20; revision received August 22; accepted August 28. **Address reprint requests to** W.G.B.

[2] Current address: Section of Neuroradiology, University of Utah, Salt Lake City.

William G. Bradley Jr, MD, PhD, gets research support from GE Medical Systems and Siemens Medical Systems.

Abbreviations: CSF = cerebrospinal fluid, FISP = fast imaging with steady-state precession, NPH = normal-pressure hydrocephalus, VP = ventriculoperitoneal.

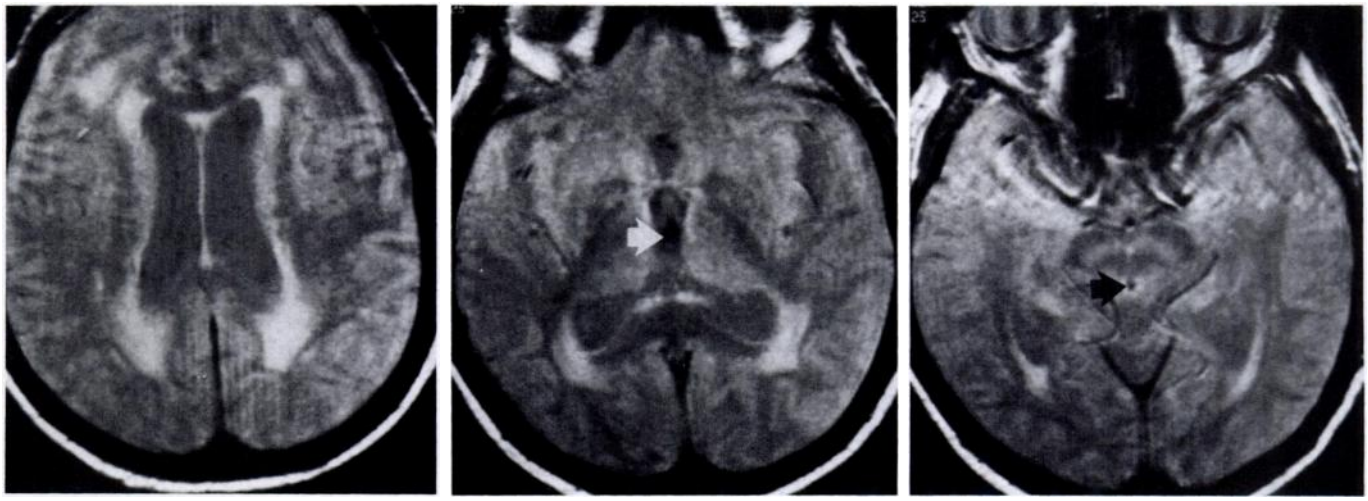

a. b. c.

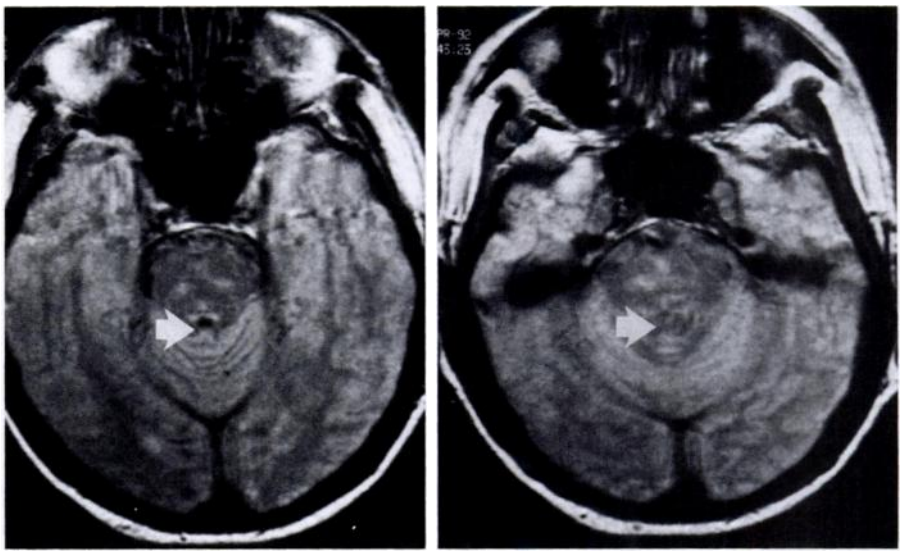

d. e.

Figure 1. Images and data obtained in an 83-year-old man (patient 8) with clinical NPH, intermediate CSF flow void, elevated aqueductal CSF stroke volume (82 μL), and favorable response to VP shunting. **(a–e)** Proton-density–weighted axial spin-echo MR images (3,000/22) demonstrate a moderate (score of 2) CSF flow void (arrow in **b–d**). *(Fig 1 continues.)*

To rectify these shortcomings, a technique has been developed that directly quantifies the volume of CSF flowing through the aqueduct. Previous studies have shown that this CSF motion is pulsatile, with a small net craniocaudal component; the parameter we measured was the aqueductal CSF stroke volume. This is defined as the average of the volume of CSF moving craniocaudad during systole and that moving caudocraniad during diastole. It is derived from measurements on phase-contrast CSF velocity MR images (26). Specifically, it is the product of the measured velocity of a pixel (in millimeters per second) and the area of that pixel (in square millimeters) integrated over the cross-sectional area of the aqueduct integrated in time over mechanical systole or diastole.

The units of the aqueductal CSF stroke volume are thus cubic millimeters or microliters. The purposes of this study were to compare the efficacies of using measurements of aqueductal CSF stroke volume and aqueductal CSF flow void on routine MR images as predictors of shunt response in patients with clinical NPH.

MATERIALS AND METHODS

In 42 consecutive patients with clinical, lumbar puncture, and routine MR imaging findings suggestive of NPH, aqueductal CSF stroke volumes were measured by means of CSF velocity MR imaging. Of these 42 patients, 18 underwent ventriculoperitoneal (VP) shunt formation because of the results of the CSF flow study, severity of NPH symptoms, and presence of coexisting disease. The study population comprises eight men and 10 women aged 54–83 years (mean age, 73 years).

Spin-echo, proton-density–weighted axial MR imaging was performed with either a 1.5-T Siemens Magnetom 63SP or SP4000 (3,000/22 [repetition time msec/echo time msec]; Siemens Medical Systems, Erlangen, Germany) or a 1.5-T GE Signa Advantage 5x (3,000/30; GE Medical Systems, Milwaukee, Wis). Imaging parameters were a standard 192 × 256 matrix, a 22-cm field of view, 20 sections, and a 5-mm section thickness. Intersection gap was 1.5 or 2.5 mm for the Siemens or GE system, respectively. First-order flow compensation in the readout and section-select directions was used in all sequences. Aqueductal flow voids were scored blindly (Table 1) by an MR imaging–trained radiologist (D.S.) on a scale of 0–4 (Figs 1–3) according to a method similar to that used in a previous study (25): 0 indicated no signal loss; 1, signal loss confined to the aqueduct and upper fourth ventricle; 2, signal loss extending from the posterior third to the upper fourth ventricles; 3, signal loss extending to the posterior third ventricle and middle fourth ventricle; and 4, signal loss extending from the foramen of Monro to the obex of the fourth ventricle. In the previous study (25), flow voids were scored as 0 and 1 in healthy control subjects and in patients who did not respond to shunting, while prominent flow voids were scored as 2–4 in patients with NPH who responded to shunting.

The techniques for CSF velocity MR imaging used in the current study have been described in detail previously (26). All CSF flow MR studies were performed with the Siemens system by using a modified, two-dimensional, fast imaging with steady-state precession (FISP) sequence (100/16; flip angle, 15°) with a section thickness of 4 mm and positioning of the section perpendicular to the aqueduct (Fig 1). Flow encoding was used in the section-select direction by using an aliasing velocity of 200 mm/sec. A 512 × 512 matrix and a 160-mm field of view were used, which resulted in an in-plane spatial resolution of 0.3125 mm. The loss of signal-to-noise ratio resulting from use of such small pixels was

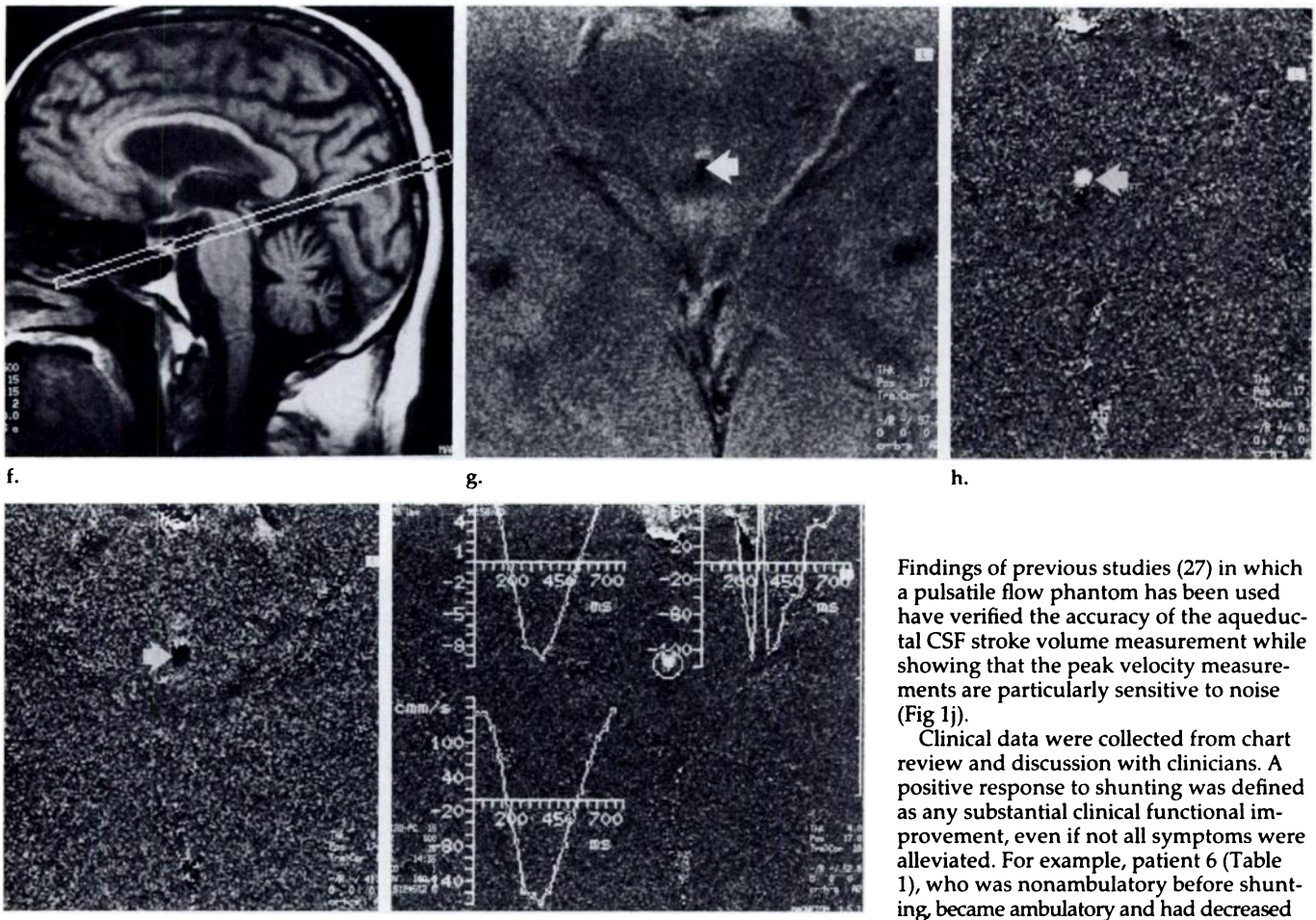

Figure 1 *(continued).* **(f)** Sagittal, scout, T1-weighted, spin-echo MR image (500/15) demonstrates position of section for assessing CSF flow through the aqueduct. **(g)** Magnitude FISP MR image (100/16; 15° flip angle) obtained during CSF flow study demonstrates aqueduct (arrow). **(h)** Phase-contrast FISP MR image (100/16; 15° flip angle) obtained during systole demonstrates craniocaudal flow (arrow; whitest areas = 200 mm/sec craniocaudal). **(i)** Phase-contrast FISP MR image (100/16; 15° flip angle) obtained during diastole demonstrates caudocranial flow (arrow; blackest areas = 200 mm/sec caudocranial). **(j)** Plots of mean velocity (millimeters per second; upper left), peak velocity (millimeters per second; upper right), and volumetric flow rate (cubic millimeters per second; lower left) as functions of the cardiac cycle (milliseconds). Peak velocity plot demonstrates aliasing.

partially compensated for by reducing the bandwidth from 130 Hertz per pixel to 78 Hertz per pixel. Use of a half-Fourier algorithm (with 16 lines of oversampling) helped to keep the measurement time within reason (14 minutes). The CSF velocity data ultimately used to calculate the aqueductal CSF stroke volume were obtained from these images.

Continuous data acquisition and retrospective cardiac gating with electrocardiographic leads were used to allow evaluation of CSF velocity during the entire cardiac cycle (26). Thirty-two flow-encoded acquisitions were obtained in 3.2 seconds (usually three or four cardiac cycles) before advance of the phase-encoding gradient. Data were then retrospectively sorted into 18 cine frames spanning the complete cardiac cycle. A "zero-velocity" reference image was calculated by averaging all the phase measurements on each of the phase images with the assumption of zero net flow through the aqueduct of Sylvius during one cardiac cycle. The phase measurements on this zero-velocity reference image were then subtracted from the phase measurements on each of the phase images to produce 18 phase-contrast, CSF velocity MR images. While this assumption of zero net flow clearly introduces some error, the magnitude of the error has been shown to be less than 5% in healthy control subjects and considerably less than 5% in patients with hydrocephalus, because more than 95% of the volumetric flow during one cardiac cycle is to-and-fro (26).

Software was developed to determine the mean and peak velocities and the volumetric flow rate through the aqueduct as a percentage of the cardiac cycle (Figs 1j, 2f, 3f). Stroke volumes for both diastole and systole were then calculated by integrating the area under the volumetric flow rate curve versus time. The mean of the absolute value of these two measurements was the aqueductal CSF stroke volume. Findings of previous studies (27) in which a pulsatile flow phantom has been used have verified the accuracy of the aqueductal CSF stroke volume measurement while showing that the peak velocity measurements are particularly sensitive to noise (Fig 1j).

Clinical data were collected from chart review and discussion with clinicians. A positive response to shunting was defined as any substantial clinical functional improvement, even if not all symptoms were alleviated. For example, patient 6 (Table 1), who was nonambulatory before shunting, became ambulatory and had decreased urinary incontinence after surgery. Although this patient had no improvement in his substantial dementia, these other improvements allowed his family to provide care at home and alleviated the need for skilled nursing. Thus, this was considered a positive outcome. This mixed response, however, was atypical. In most patients, there was either obvious improvement or clearly no substantial change; thus, differentiation between positive and negative responses to shunting was, in most cases, not difficult.

RESULTS

The routine MR images obtained in all patients displayed ventriculomegaly, usually out of proportion to sulcal enlargement (although varying degrees of atrophy were also present). Age, sex, aqueductal CSF flow void score, aqueductal CSF stroke volume, and response to shunting are summarized in Table 1.

All 12 patients in this series with stroke volumes greater than 42 μL responded to shunting (Fig 1), while half of the six patients with an aqueductal CSF stroke volume of 42 μL or less did not respond (Figs 2, 3). Patients with an aqueductal CSF stroke volume greater than 42 μL were, therefore, considered to have hyperdynamic CSF flow and positive CSF flow study findings, while those with

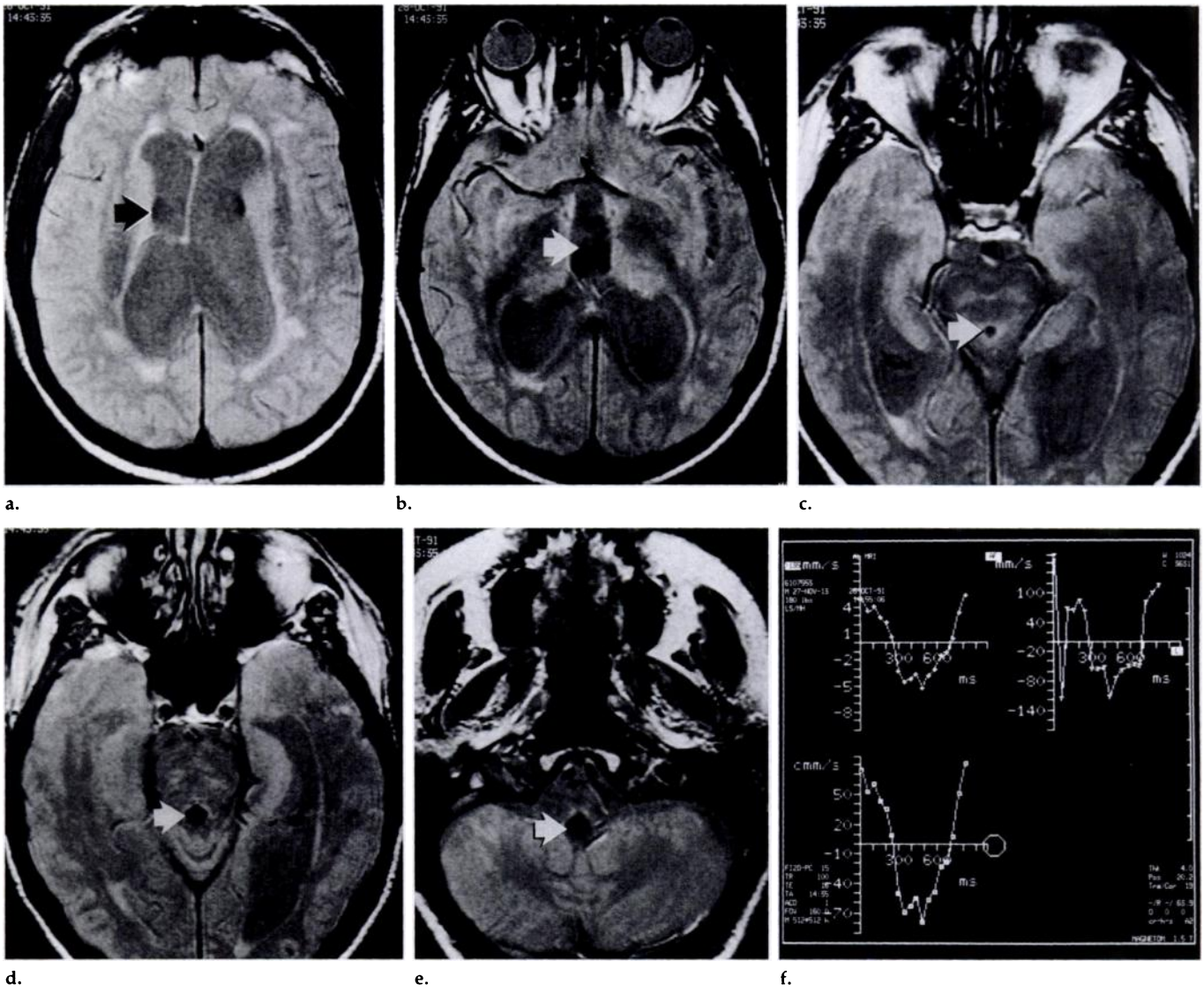

Figure 2. Images and data obtained in a 77-year-old man (patient 11) with increased CSF flow void; borderline, decreased aqueductal CSF stroke volume (42 μL); and negative response to VP shunting. **(a–e)** Proton-density–weighted axial spin-echo MR images (3,000/22) demonstrate marked CSF flow (score of 4) through aqueduct and third and fourth ventricles (arrow). **(f)** Plot of mean velocity (millimeters per second) and volumetric flow rate (cubic millimeters per second) as a function of the cardiac cycle (milliseconds). Velocity is substantially reduced compared with that in the patient in Figure 1, who had hyperdynamic flow.

an aqueductal CSF stroke volume less than 42 μL were considered to have normal CSF flow and negative CSF flow study findings. Of the 12 patients with positive study findings, all improved after CSF diversion; thus, positive predictive value was 100%. Three of the patients with negative CSF flow study findings responded positively to shunting, while three did not respond; thus, negative predictive value was 50%.

The sensitivity of the aqueductal stroke volume criteria was 80%, and the specificity was 100%. Overall accuracy was 83%. These results are summarized in Tables 2 and 3. Results of a Fisher exact test performed with the data in Table 2 indicate a significant association between high CSF stroke volume and favorable surgical response ($P < .05$).

As in a previous study (25), all patients with CSF flow void scores of 2 or higher were considered to have hyperdynamic CSF flow and positive study findings, while those with a score of 0 or 1 were considered to have normal CSF flow and negative study findings. Of the 12 patients with positive findings according to these criteria, 11 had improvement with CSF shunting (Fig 1) while one did not (Fig 2). In contrast, four of the patients with negative findings had improvement while two did not (Fig 3). These data are listed in Table 4; there was no statistically significant relationship between the CSF flow void score and response to CSF shunting according to Fisher exact test results. The sensitivity of using these CSF flow void score criteria was 73%; specificity, 67%; positive predictive value, 92%; and negative predictive value, 33%. Overall accuracy was 72%. These results are summarized in Table 3.

DISCUSSION

The following conclusions can be drawn from this study. Positive CSF flow study findings (ie, stroke volume greater than 42 μL) are associated with an increased likelihood of improvement with CSF shunting. Positive predictive value in the patients in this study was 100%. Negative predictive value of the quantitative CSF flow study findings was 50%. Positive predictive value for the CSF flow void score was 92%; thus, when findings are positive, there is a reasonable

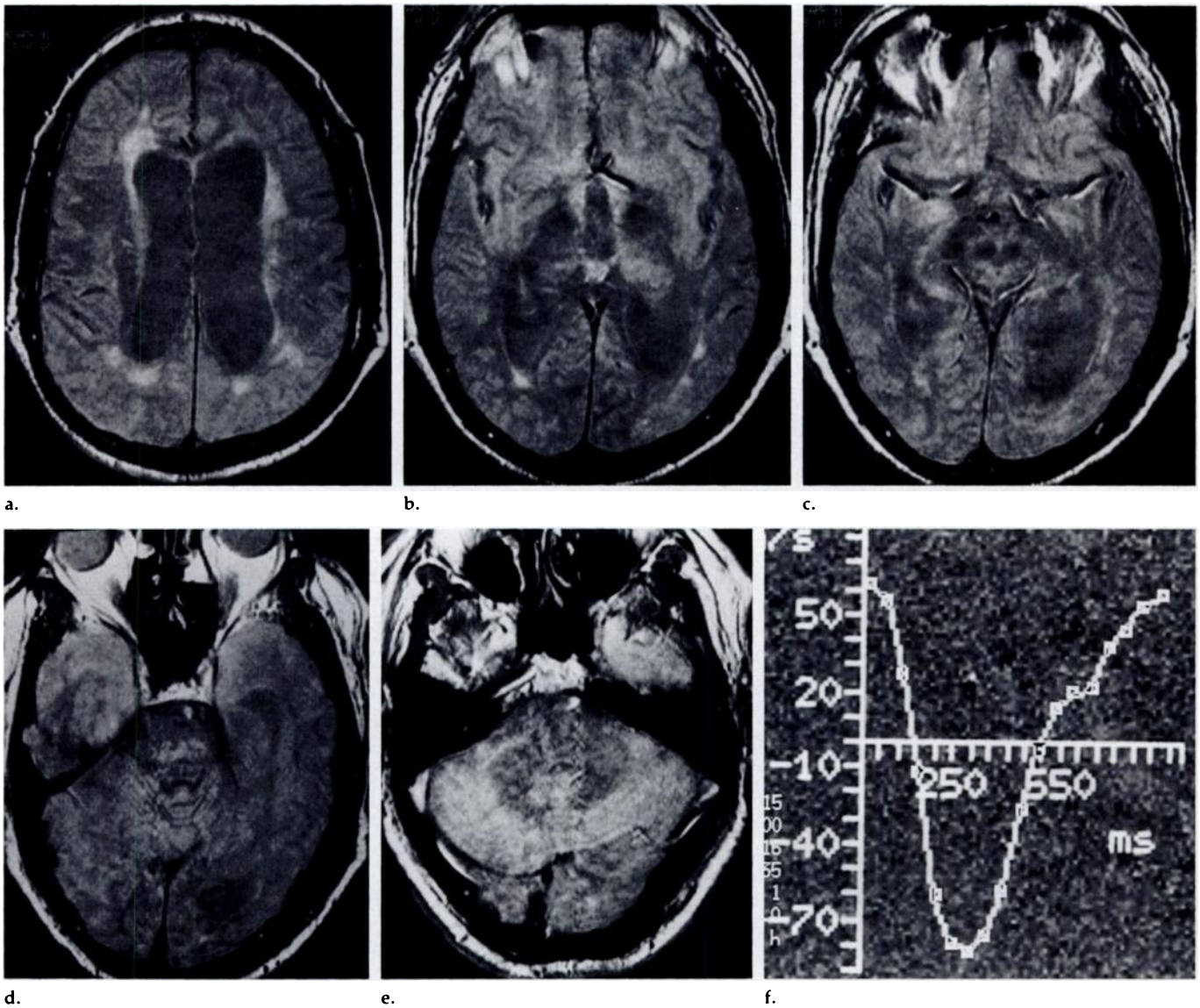

Figure 3. Images and data obtained in a 69-year-old man (patient 18) with minimal CSF flow void (score of 1) and decreased aqueductal CSF stroke volume (38 μL) consistent with atrophy who nonetheless underwent shunt formation without response. **(a–e)** Proton-density–weighted axial spin-echo MR images (3,000/22) demonstrate minimal CSF flow void. **(f)** Plot of volumetric flow rate versus phase of the cardiac cycle shows decreased flow compared with that in Figure 1. X axis indicates milliseconds, and y axis indicates cubic millimeters or microliters per second.

chance of a favorable surgical response. Negative predictive value for the CSF flow void score was only 33%. Thus, when a marked flow void is not seen, the patient may still have a favorable response to surgery. This probably represents CSF motion averaging during the cardiac cycle in a patient with an elevated aqueductal CSF stroke volume. Overall, the quantitative aqueductal CSF stroke volume is a better predictor than the qualitative CSF flow void score.

That the aqueductal CSF stroke volume was more sensitive to hyperdynamic flow than the CSF flow void score was predictable. The aqueductal CSF flow void represents an average of CSF motion during the entire cardiac cycle. The aqueductal CSF stroke volume, on the other hand, is derived from cardiac-gated data without averaging over systole and diastole. Before the use of flow compensation, aqueductal CSF flow resulted in relatively greater signal loss. With the routine use of flow-compensation techniques, the aqueductal flow void is less prominent, and the CSF flow void sign previously reported (25) has become a less sensitive predictor of NPH response to ventricular shunting.

Understanding the association between elevated CSF stroke volume and favorable shunt response requires knowledge of the underlying cause of NPH. Unfortunately, this pathophysiology has eluded investigators since the initial description of the disease. Indeed, multiple explanations have been put forth, none of which is entirely adequate. However, one model previously described (25) explains much of what is seen in the current study and is compatible with many of the theories and phenomena described in the literature.

As originally conceived (25), the primary purpose of CSF flow analysis was to differentiate shunt-responsive NPH from cerebral atrophy ("burned out" NPH). Both conditions are characterized by ventriculomegaly; however, the latter does not respond to CSF diversion.

In the setting of NPH, the brain is pushed close to the cranium because of ventricular enlargement. During systole, blood fills the cerebral hemi-

spheres. Because the brain cannot expand outward, it expands inward. This compresses the lateral and third ventricles, expressing a relatively large volume of CSF through the aqueduct. This results in a prominent CSF flow void and a large CSF stroke volume. Roughly the same volume of CSF returns to the lateral ventricles during diastole with egress of blood from the cranial vault through the venous system. In atrophy, by comparison, blood flow to the brain is decreased; thus, stroke volume is smaller and there is a reduced CSF flow void.

It is generally accepted that NPH-like symptoms are produced when the expanded lateral ventricles place excessive tangential shearing forces on periventricular white matter fibers associated with gait; problem with gait is often the primary symptom in NPH. With continued ventricular expansion, the cortex is exposed to increased radial shearing forces, leading to dementia. Recent preliminary MR imaging studies depicting brain motion (28) hold promise for the evaluation of such shearing motions. Indeed, abnormal findings have been documented at histopathologic analysis and MR imaging in the periventricular region in patients with NPH (29–31). Some authors have implicated compromised cerebral blood flow as the main contributing factor to these histopathologic changes (31–35).

Pettorossi et al (36) placed latex balloons in the lateral ventricles of lambs posterior to the foramen of Monro. They inflated and deflated them synchronously with normal CSF pulsations such that the CSF pulse pressure was increased without a concomitant increase in the mean CSF pressure—a situation analogous to that seen in NPH (36,37). A second group of animals underwent similar inflation and deflation of a balloon within the brain parenchyma, while a third group underwent permanent inflation of balloons (without pulsation) in both lateral ventricles. In only the first group, in which the elevated CSF pulse pressure originated from within the lateral ventricles, did periventricular histopathologic changes such as those reported in patients with NPH manifest. Thus, it was concluded that the critical factor responsible for symptoms in NPH was the "waterhammer" force exerted by the reexpanding lateral ventricles on the periventricular tissues. The purpose of shunting in such patients was, therefore, not to decrease the mean pressure (which was already normal), but rather to provide additional capacitance. Thus, when the brain expands during systole, some of the CSF can go out the shunt, limiting the maximum pressure rise and the shearing forces on the periventricular fibers.

One must explain why some patients with imaging findings suggestive of atrophy have improvement after CSF shunting (7). To do this, one must consider that both the CSF stroke volume and CSF pulse pressure are influenced not only by the degree of atrophy present, but also by the ventricular size, aqueductal diameter, brain compliance, and cerebral blood flow. For example, compromised microvasculature in the periventricular region might allow these tissues to become injured at a lower pulse pressure than would tissues with a normal microvascular supply (31). Alternatively, decreased tensile strength of the ventricular wall or adjacent parenchyma might allow greater diastolic reexpansion of the ventricles (32–42), leading to increased mechanical trauma to the periventricular white matter tracts and/or increased transependymal CSF flow. This would cause decreased tissue pressure and microvascular compromise (35).

Several limitations of this study should be noted. First, the number of patients, especially those with negative CSF flow study findings who underwent shunt formation, is small. Second, the study is retrospective. (A prospective trial in which all patients undergoing a quantitative CSF flow study, including those thought not to have NPH, also would undergo shunt formation would be difficult to justify ethically.) Third, although attempts were made at blinding chart reviews, this was not always possible because of information about the CSF flow study written in the physician's notes. Fourth, although this phase-contrast technique is excellent for quantitating laminar flow (27), it may result in substantial underestimation of turbulent flow in patients with especially hyperdynamic CSF flow. Fortunately, in such cases, the CSF flow void should be particularly prominent.

Despite these shortcomings, it is thought that the quantitative CSF flow study is a useful method of predicting response to shunting in patients with NPH and should be considered the test of choice after clinical evaluation and routine imaging (ie, computed tomography or MR imaging) in the work-up in such patients. ■

Table 2
Response to Shunt according to Quantitative CSF Flow Study Results

Clinical Response to Shunt	No. of Patients with Stroke Volume	
	>42 μL	≤42 μL
Improvement	12	3
No improvement	0	3

Note.—Positive result was defined as a stroke volume >42 μL; a negative result, ≤42 μL. $P < .05$ according to the Fisher exact test.

Table 3
Sensitivity, Specificity, Predictive Values, and Accuracy of Results of Quantitative CSF Flow Study versus CSF Flow Void Analysis

Parameter	Quantitative CSF Flow Study Results	Flow Void Analysis Results
Sensitivity (%)	80	73
Specificity (%)	100	67
Positive predictive value (%)	100	92
Negative predictive value (%)	50	33
Accuracy (%)	83	72

Table 4
Response to Shunt according to CSF Flow Void Score

Clinical Response to Shunt	No. of Patients with CSF Flow Void Score	
	≥2	<2
Improvement	11	4
No improvement	1	2

Note.—A flow void score of ≥2 or greater indicated hyperdynamic CSF flow; a score of <2 indicated normal CSF flow. Differences were not statistically significant according to the Fisher exact test.

References

1. Hakim S, Adams RD. The special clinical problem of symptomatic hydrocephalus with normal cerebrospinal fluid pressure: observations on cerebrospinal fluid hydrodynamics. J Neurol Sci 1965; 2:307–327.
2. Adams RD, Fisher CM, Hakim S, et al. Symptomatic occult hydrocephalus with "normal" cerebrospinal fluid pressure. N Engl J Med 1965; 273:117–126.
3. Black PN. Idiopathic normal-pressure hydrocephalus: results of shunting in 62 patients. J Neurosurg 1980; 53:371–377.
4. Black PN, Ojemann G, Tsouras A. Cerebrospinal fluid shunts for dementia, gait disturbance, and incontinence. Clin Neurosurg 1985; 32:632–656.
5. Greenberg JO, Shenkin HA, Adam R. Idiopathic normal pressure hydrocephalus: a report of 73 patients. J Neurol Neurosurg Psychiatry 1977; 40:336–341.

6. Laws ER, Mokri B. Occult hydrocephalus: results of shunting correlated with diagnostic tests. Clin Neurosurg 1977; 24:316–333.
7. Black PN, Ojemann RG. Hydrocephalus in adults. In: Youmans JT, ed. Neurological surgery. New York, NY: Saunders, 1990; 1284–1298.
8. Vanneste J, Augustijn P, Dirven C, Tan WF, Goedhart ZD. Shunting normal-pressure hydrocephalus: do the benefits outweigh the risks? A multicenter study and literature review. Biology 1992; 42:54–59.
9. Fisher CM. The clinical picture in occult hydrocephalus. Clin Neurosurg 1977; 24: 270–284.
10. Jacobs L, Conti D, Kinkel WR. Normal-pressure hydrocephalus. Relationships of clinical and radiologic findings to improvement following shunt surgery. JAMA 1976; 235:510–512.
11. Vassiloughis J. The syndrome of normal-pressure hydrocephalus. J Neurosurg 1984; 61:501–509.
12. Borgsen SE, Gjerris F, Sorensen SC. Cerebrospinal fluid conductance and compliance of the cranial spinal space in normal pressure hydrocephalus. J Neurosurg 1979; 51:521–525.
13. Borgsen SE, Gjerris F. The predictive value of conductance to outflow of cerebrospinal fluid in normal pressure hydrocephalus. Brain 1982; 105:65–86.
14. Nelson JR, Goodman SJ. An evaluation of the cerebrospinal fluid infusion test for hydrocephalus. Neurology 1971; 21:1037–1053.
15. Wikkelso C, Andersson H, Blomstrand C. The clinical effect of lumbar puncture in normal pressure hydrocephalus. J Neurol Neurosurg Psychiatry 1982; 45:64–69.
16. Heinz ER, Davis DO, Carp HR. Abnormal isotope cisternography and symptomatic occult hydrocephalus: a cooperative isotopic-neuroradiologic study in 130 patients. Radiology 1970; 95:109–120.
17. Tator CH, Murray SA. A clinical, pneumoencephalographic and radio-isotope study of normal-pressure communicating hydrocephalus. Can Med Assoc J 1971; 105: 573–579.
18. Jacobs L, Kinkel WR. Computerized axial transverse tomography and normal pressure hydrocephalus. Neurology 1976; 26: 501–507.
19. Drayer BP, Rosenbaum AE. Dynamics of cerebrospinal fluid system as defined by cranial computed tomography. In: Wood JH, ed. Neurobiology of cerebrospinal fluid. Vol 1. New York, NY: Plenum, 1980.
20. Greitz TVB, Grepe OAL, Kalmer MSF, Lopez, J. Pre- and postoperative evaluation of cerebral blood flow in low-pressure hydrocephalus. J Neurosurg 1969; 31:644–651.
21. Grubb RL, Raichle ME, Gado MH, Eichling JO, Hughes CP. Cerebral blood flow, oxygen utilization and blood volume in dementia. Neurology 1977; 27:905–910.
22. Mathew NT, Meyer JS, Hartmann A, Ott EO. Abnormal cerebrospinal fluid–blood flow dynamics: implications in diagnosis, treatment, and prognosis in normal pressure hydrocephalus. Arch Neurol 1975; 32:657–664.
23. Meyer JS, Kitagaura Y, Tanabashi N, et al. Evaluation of treatment of normal pressure hydrocephalus. J Neurosurg 1985; 62:513–521.
24. Meyer JS, Kitagaura Y, Tanabashi N, et al. Pathogenesis of normal pressure hydrocephalus: preliminary observations. Surg Neurol 1985; 23:121–133.
25. Bradley WG, Whittemore AR, Kortman KE, et al. Marked cerebrospinal fluid void: indicator of successful shunt in patients with suspected normal-pressure hydrocephalus. Radiology 1991; 178:459–466.
26. Nitz WR, Bradley WG, Watanabe AS, et al. Flow dynamics of cerebrospinal fluid: assessment with phase-contrast velocity MR imaging performed with retrospective cardiac gating. Radiology 1992; 183:395–405.
27. Mullin WJ, Atkinson D, Hashemi RH, Yu J, Bradley WG. High resolution quantitative assessment of aqueductal CSF motion by phase contrast MRI technique: correlation with pulsatile flow phantom. JMRI 1993; 3:55.
28. Enzmann DR, Pelc NJ. Brain motion: measurement with phase contrast MR imaging. Radiology 1992; 185:653–658.
29. DeLand FH, James AE Jr, Ladd DJ, et al. Normal pressure hydrocephalus: a histologic study. Am J Clin Pathol 1972; 58:58–63.
30. Di Rocco C, Di Trapani J, Maira G, et al. Anatomic-clinical correlations in normal tensive hydrocephalus: reports on 3 cases. J Neurol Sci 1977; 33:436–452.
31. Bradley WG, Whittemore AR, Watanabe AS, Davis SJ, Teresi LM, Homyak M. Association of deep white infarction with chronic communicating hydrocephalus: implications regarding the possible origin of normal-pressure hydrocephalus. AJNR 1991; 12:31–39.
32. Greitz T. Effect of brain distention on cerebral circulation. Lancet 1969; 1:863–865.
33. Greitz TVB, Grepe AOL, Kalmer MSF, Lopez J. Pre- and postoperative evaluation of cerebral blood flow and low pressure hydrocephalus. J Neurosurg 1969; 31: 644–651.
34. Mathew NT, Meyer JS, Hartmann A, Ott EO. Abnormal cerebrospinal fluid–blood flow dynamics: implications in diagnosis, treatment, and prognosis in normal pressure hydrocephalus. Arch Neurol 1975; 32:657–664.
35. Meyer JS, Kitagawa Y, Tanahashi N, et al. Pathogenesis of normal pressure hydrocephalus: preliminary observations. Surg Neurol 1985; 23:121–133.
36. Pettorossi VE, Di Rocco C, Mancinelli R, Caldareli M, Velardi F. Communicating hydrocephalus induced by mechanically increased amplitude of the intraventricular cerebrospinal fluid pulse pressure: rationale and method. Exp Neurol 1978; 59:30–39.
37. Sato K, Fuchinoue T, Yahagi Y. CSF pulse wave changes in cases with normal pressure hydrocephalus. In: Lundberg N, Ponten U, Brock M, eds. Intracranial pressure. Vol 2. New York, NY: Springer-Verlag New York, 1975; 133–136.
38. Di Rocco C. Hydrocephalus and cerebrospinal fluid pulses. In: Shapiro K, Marmarou A, Portnoy H, eds. Hydrocephalus. New York, NY: Raven, 1984; 231–249.
39. Foltz EL, Aine C. Diagnosis of hydrocephalus by CSF pulse-wave analysis: a clinical study. Surg Neurol 1981; 15:283–293.
40. Sklar FH, Diehl JT, Beyer CW Jr, Clark WK. Brain elasticity changes with ventriculomegly. Gen Neurosurg 1980; 53:173–179.
41. Tamaki N, Kusunoki T, Wakabayashi T, Matsumoto S. Cerebral hemodynamics in normal-pressure hydrocephalus. Gen Neurosurg 1984; 61:510–514.
42. Ingvar DH, Schwartz MS. The cerebral blood flow in low pressure hydrocephalus. In: Lundberg N, Ponten U, Brock M, eds. Intracranial pressure. Vol 2. New York, NY: Springer-Verlag New York, 1975; 153–156.